

# Clearing of polydisperse water aerosol upon thermal blooming of a slit laser beam

A.N. Kucherov

*N.E. Zhukovskii Central Aerohydrodynamical Institute, Zhukovskii, Moscow Region*

Received December 27, 2005

The water aerosol (fogs and clouds) clearing under conditions of the thermal blooming of a laser beam vaporizing particles is under study. The diffraction spreading, relative motion of the beam and the medium, absorption and scattering of the radiation, and the particle size distribution are taken into account. The transparency function is investigated in dependence of the initial optical thickness, clearing and thermal blooming parameters, and the Fresnel number for a slit beam. The comparison with experimental data is carried out.

## Introduction

With the advent of lasers, the problem of the aerosol optical density decreasing through vaporizing particles in a wide range of energy densities (from the solar one to the threshold of the gas breakdown) and temperatures (from the air temperature to the water critical temperature, at which drops explode) has become urgent.<sup>1-4</sup> Depending on the vapor speed at the outer boundary of the Knudsen layer, different vaporization modes are realized on the particle surface: diffusion, diffusion-convective, subsonic, sonic, and explosive.<sup>5</sup> We study the clearing at low vaporization rates: the diffusion and diffusion-convective modes. The problem includes a macroscale of the order of the beam radius  $r_0$  and a microscale of the order of the droplet radius  $a$ .

Earlier the complex multiparametric problem of the clearing was solved with significant simplifications: the approximation of a homogeneous optical field inside a particle (used by us too), the linear dependence of factors of radiation absorption and extinction at an individual droplet (fine aerosol approximation), quasistationary temperature in the process of the considerable decrease of the particle size due to vaporization, constant efficiency of vaporization (the fraction of the radiation energy absorbed by a particle, which goes to the vaporization), approximation of the liquid-water content function, at which the attenuating action of the aerosol upon the radiation is characterized by the function, smooth within the scale of the beam radius.

For estimates, as well as approximate and more accurate calculations, it is important to find the domain of validity of the above assumptions. This allows obtaining solutions under more rigorous formulation of the problem. The physical similarity and the separation of dimensionless parameters responsible for some or other physical phenomena (diffraction, radiation absorption and extinction, thermal blooming of a beam, heating and vaporization of particles, aerosol medium clearing) lead to a

significantly smaller number of parameters, affecting main characteristics of the beam and aerosol medium. In this paper, the clearing process is studied under conditions of strong thermal blooming or self-refraction.

## 1. Formulation of the problem

1. Laser radiation propagation in aerosol is described on the macroscale by the equation for a slowly varying transversal component of the electric field  $E$  amplitude<sup>6</sup> (intensity  $I = EE^*$ ):

$$-2ik_\lambda n_0 \frac{\partial E}{\partial z} + \frac{\partial^2 E}{\partial x^2} + \left[ 2k_\lambda^2 n_0 (n_0 - 1) \frac{\rho - \rho_0}{\rho_0} E - i\alpha k_\lambda n_0 E \right] = 0, \quad (1)$$

$$E|_{z=0} = E_0(x), \quad E|_{x \rightarrow \pm\infty} \rightarrow 0;$$

$$h_0 \left[ \frac{\partial(\rho - \rho_0)}{\partial t} + V_0 \frac{\partial(\rho - \rho_0)}{\partial x} \right] = -\alpha_* I, \quad (2)$$

$$\rho|_{t=0} = \rho_0, \quad \rho|_{x \rightarrow -\infty} \rightarrow \rho_0,$$

where  $z, x$  are longitudinal and transversal coordinates with respect to the beam;  $t$  is time;  $k_\lambda = 2\pi/\lambda$  is the wave number;  $n_0$  is the refractive index of the unperturbed gas;  $\rho, \rho_0$  are the gas density and its initial unperturbed value;  $h_0$  is the enthalpy of the unperturbed gas;  $V_0$  is the speed of the transversal flow;  $\alpha_{\text{ext}}, \alpha_{\text{abs}}$  are the linear coefficients of the radiation extinction and absorption by the aerosol;  $\alpha_* = \alpha_{\text{abs}}\eta$  is the effective coefficient of the radiation absorption by the gas;  $\eta$  is the fraction of the absorbed by aerosol energy going to the gas. Without loss in generality, consider a plane beam with the Gaussian initial field distribution

$$E_0(x) = \sqrt{I_0} \exp[-(x/r_0)^2/2],$$

where  $I_0 = P_0/\pi r_0^2$  is the characteristic intensity;  $P_0$  is the total power;  $r_0$  is the exponential beam radius.

The aerosol absorption  $\alpha_{\text{abs}}$  and extinction  $\alpha_{\text{ext}}$  coefficients are calculated on the basis of the Mie theory<sup>7</sup>:

$$\alpha_i(x, z, t) = \pi N \int_0^\infty a^2 Q_i(a) f(x, z, t, a) da, \quad i = \text{abs, ext.} \quad (3)$$

Here  $Q_{\text{abs}}$ ,  $Q_{\text{ext}}$  are factors of radiation absorption and extinction at a sphere of the radius  $a$ ;  $f(x, z, t, a)$  is the particle size distribution function;  $N$  is the number of particles in the unit volume.

It should be noted that, in the fine aerosol approximation ( $a \rightarrow 0$ ), the linear approximation is usually applied to  $Q_{\text{abs}}$ ,  $Q_{\text{ext}}(a)$ . Actually, as was shown by the rigorous calculations, the ratio  $Q_{\text{ext}}(a)/Q_{\text{abs}}(a)$  is not constant (see, e.g., Ref. 3, p. 144).

2. On the macroscale, the evolution of the droplet radius  $a$ , temperature  $T$ , and the distribution function  $f(x, z, t, a)$  in the space of independent variables (the spectrum of radii  $a$ , longitudinal  $z$  and transversal  $x$  coordinates, time  $t$ ) is described by equations<sup>1-4</sup>

$$\frac{\partial a}{\partial t} + V_0 \frac{\partial a}{\partial x} = -\frac{j}{\rho_w}, \quad a|_{t=0, x \rightarrow -\infty} = a_0; \quad (4)$$

$$\rho_w C_w \left[ \frac{\partial T}{\partial t} + V_0 \frac{\partial T}{\partial x} \right] = \alpha_d I(x, z, t) - \frac{3}{a} [j H_w + j_T], \quad (5)$$

$$T|_{t=0, x \rightarrow -\infty} = T_\infty;$$

$$\frac{\partial f}{\partial t} + V_0 \frac{\partial f}{\partial x} + \frac{\partial}{\partial a} \left[ f \frac{da}{dt} \right] = 0, \quad (6)$$

$$f|_{t=0, x \rightarrow -\infty} = f_0(a_0) \equiv \frac{\mu^{\mu+1} a_0^\mu}{\Gamma(\mu+1) a_m^{\mu+1}} e^{[-\mu a_0/a_m]}.$$

Here  $j$ ,  $j_T$  are the densities of the mass and heat fluxes from the droplet surface;  $\rho_w$ ,  $C_w$ ,  $H_w$  are the density, specific heat, and specific heat of water evaporation;  $a_0$ ,  $T_\infty$  are the droplet initial radius and the temperature, equal to the temperature of the ambient medium;  $\alpha_d = 3Q_{\text{abs}}/4a$  is the volume-averaged coefficient of the radiation absorption by the droplet;  $f_0(a_0)$  is the initial two-parameter gamma distribution with the parameters  $\mu$  and  $a_m$  (modal and most probable radius). The densities of the mass and heat fluxes from the particle surface have the form

$$j = \begin{cases} \frac{\langle \rho D \rangle}{a} \ln \left[ \frac{1 - Y_\infty}{1 - Y} \right], & T < T^*, \\ \rho_K u_K, & T \geq T^* \end{cases}, \quad Y_\infty \cong \frac{p_{s\infty} m_v}{\rho_\infty m}, \quad (7)$$

$$j_T = \begin{cases} -\langle k \rangle \frac{\partial T}{\partial r} \Big|_{r=a} = j \langle k \rangle \left\langle \frac{C_p}{k} \right\rangle \frac{T - T_\infty}{\exp(ja \langle C_p/k \rangle) - 1}, & T < T^*, \\ \rho_K u_K \left[ h_K(T_K) - h_s(T) + \frac{u_K^2}{2} \right], & T \geq T^*. \end{cases} \quad (8)$$

The brackets  $\langle \dots \rangle$  denote the temperature averaging of the vapor diffusion coefficient  $D$ , the gas specific heat  $C_p$ , and the thermal conductivity coefficient  $k$  of

air;  $Y = \rho_v/\rho$ ,  $Y_\infty$  are the relative mass concentration of the vapor and its value in the ambient air;  $\rho_v$  is the vapor density;  $\rho$  is the density of the air and vapor mixture;  $p_{s\infty}$ ,  $p_\infty$  are pressures of the saturated vapor and air at  $T_\infty$ ;  $m_v$ ,  $m$  are molar masses of vapor and air;  $\rho_K$ ,  $u_K$  are the vapor density and speed at the outer boundary of the Knudsen layer<sup>8</sup>;  $h_s(T)$ ,  $h_K(T_K)$  are the enthalpy of the vapor, saturated at the droplet surface temperature  $T$ , and the enthalpy of the vapor at the top boundary of the Knudsen layer. The temperature  $T^*$  close to the boiling point separates the slow and high-speed vaporization modes. The analysis of variation of parameters throughout the droplet temperature range from the initial  $T_\infty$  to the critical value (647.3 K) has been carried out in Ref. 5. In the approximation of the liquid-water content function  $w = 4\pi\rho_w N \int a^3 f(a) da/3$  [Ref. 9], in which the details of the macroprocesses at individual particles were taken into account integrally through the solution of the transfer equation for  $w$ , the aerosol clearing under action of the thermal blooming have been studied earlier in steady-state<sup>10</sup> and unsteady<sup>11</sup> conditions.

The analysis shows that the rigorous consideration of the mass and heat fluxes from the droplet surface markedly influences physical characteristics of the process of aerosol medium clearing, namely, the radiation absorption and extinction coefficients, the aerosol layer optical thickness, and the transparency function.

## 2. Parameters of similarity

The problem includes about fifty physical dimensional parameters, while the dimensionless equations include a significantly smaller number of the similarity parameters, to be noted among which are main parameters responsible for particular physical effects: Fresnel number  $F = k_\lambda n_0 r_0^2/L$ , the aerosol extinction parameter

$$N_\alpha = \alpha_0 L,$$

where  $L$  is the path length;

$$\alpha_0 = \pi N a_m^2 Q_{\text{ext}}(a_m);$$

the thermal-blooming parameter

$$N_t = \alpha^* I_0 L^2 (n_0 - 1) / n_0 \rho_0 h_0 r_0 V_0,$$

where

$$\alpha^* = \eta_0 \pi N a_m^2 Q_{\text{abs}}(a_m), \quad \eta_0 = 1 - \eta_{v0}.$$

As a result of the clearing, the aerosol optical thickness  $\tau(x, z, t) = \int \alpha_{\text{ext}} dz$  decreases.

In place of the parameter  $N_\alpha$ , it is possible to use the equivalent parameter, i.e., the initial optical thickness  $\tau_0 = \tau(x=0, L; t=0)$ . An important role is played by the vaporization parameter  $\eta_v = j H_w / (j H_w + j_T)$ , which in the lower limit of the diffusion mode is equal to:

$$\eta_0 = \eta_{v, \text{min}} \equiv 1 / [1 + k_x T_\infty^2 m p_x R / \rho_0 D_x H_x^2 m_v^2 p_{s\infty}]$$

(according to Eqs. (7), (8)) [Refs. 1 and 12]. The parameter  $\eta_{v0}$  (and  $\eta_v$ ) depends significantly on  $T_\infty$  and  $p_\infty$  and decreases drastically when passing from the sea level to the heights  $h \geq 10$  km (Fig. 1) [Ref. 13]. As a particle heats from the initial  $T_\infty$  to  $T^*$ ,  $\eta_v$  increases from  $\eta_{v0}$  minimal value to unity. Usually, the heating of the droplet takes shorter time than its vaporization, that is,  $dT/dt \approx 0$  in the process of the clearing; and  $\eta_v$  is the radiation efficiency<sup>3,13</sup> and  $\eta = 1 - \eta_v$ .

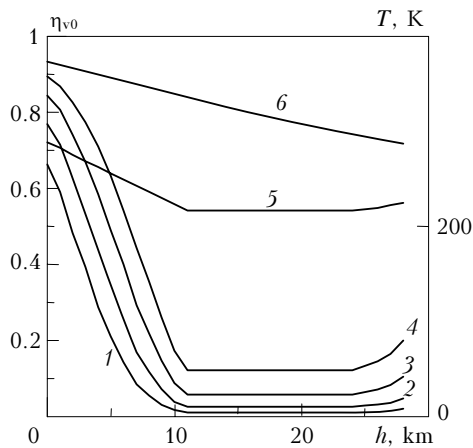


**Fig. 1.** Dependence of the minimal value of the vaporization parameter  $\eta_{v0}$  on the height above the sea level in the standard atmosphere: temperature of the ambient air around the droplet is equal to the annual average one  $T_\infty$  (curve 1);  $T_\infty + 10$  K (2);  $T_\infty + 20$  K (3);  $T_\infty + 30$  K (4); annual average temperature in the standard atmosphere  $T_\infty$ , K (5); boiling point  $T_b$ , K (6).

The clearing effect is characterized by the parameter  $N_{v0} = \alpha_{dm} I_0 \eta_{v0} r_0 / 3 \rho_w H_\infty V_0$ , entering into the dimensionless equations (4) and (6). Here  $\alpha_{dm} = \alpha_d(a_m)$  is the characteristic value of the volume-averaged coefficient of radiation absorption inside the droplet. The use of the characteristic mass and energy fluxes  $j_0 = \alpha_{dm} I_0 a_m \eta_{v0} / 3 H_\infty$ ,  $j_{T0} = j_0 H_\infty (1 - \eta_{v0}) / \eta_{v0}$  gave the same form of the clearing parameter as in approximation of the liquid-water content.<sup>10,11</sup>

### 3. Results

The system of equations (1), (4)–(6) with allowance for the relationships (3), (7), and (8) was solved numerically by the finite-difference methods with the application of the Fourier transform method. The number of nodes of the computational grid along the coordinate  $a$  amounted 40 (with minimal radii of  $0.1 a_m = \Delta a$ , and maximal ones of  $39 \Delta a$ ), the number of nodes along the coordinate  $z$  was 25, and along  $x$  from 64 to 1024. The solutions were obtained with the similarity parameter ranges  $0.5 < F \leq \infty$ ,  $0.1 \leq N_{v0} \leq 3$ ,  $0.283 \leq \tau_0 \leq 3$ ,  $0.5 \leq N_t \leq 2$ .

Let us consider the results. Figure 2 depicts the intensity distributions at the beam path end in the steady-state limit of the clearing process.

The physical parameters are the following:  $P_0 = 1$  kW,  $\lambda = 10.6$   $\mu\text{m}$ ,  $a_m = 5$   $\mu\text{m}$ ,  $\mu = 2$ , the number of particles in the unit volume  $N = 10^8$   $\text{m}^{-3}$ ,  $r_0 = 0.0076$ – $0.015$  m,  $V_0 = 0.148$ – $0.296$  m/s,  $L = 26.2$  m,  $p_\infty = 1$  atm,  $T_\infty = 288.15$  K,  $p_{s\infty} = 1704$  Pa,  $Y_\infty = 0.0104$ . The similarity parameters are given in the caption to Fig. 2. The diffraction leads only to the beam widening (curve 5), The clearing gives an increase of the intensity peak and its shift downward along the flux (curve 4). The thermal blooming (in the convective mode<sup>14</sup>) weakly defocuses the beam and shifts it to meet the flux, and both these effects increase with  $N_t$  increase.

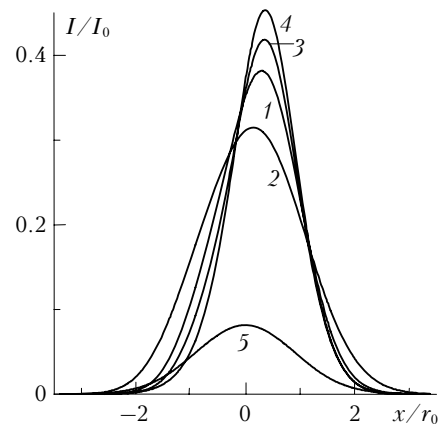


**Fig. 2.** Transversal intensity distributions of the laser beam at the path end at  $N_\alpha = 0.2$  ( $\tau_0 = 1.133$ ),  $N_{v0} = 1$ :  $N_t = 1$ ,  $F = 2.59$  (1);  $N_t = 2$ ,  $F = 1.29$  (2);  $N_t = 0.5$ ,  $F = 5.18$  (3);  $N_t = 0$ ,  $F = 5.18$  (4);  $N_t = 0$ ,  $N_{v0} = 0$ ,  $\tau_0 = 1.133$ ,  $F = 1.29$  (5).

The level of the optical thickness decrease as a result of the clearing process under the considered conditions weakly depends on the thermal-blooming parameter, as can be seen from the results depicted in Fig. 3.

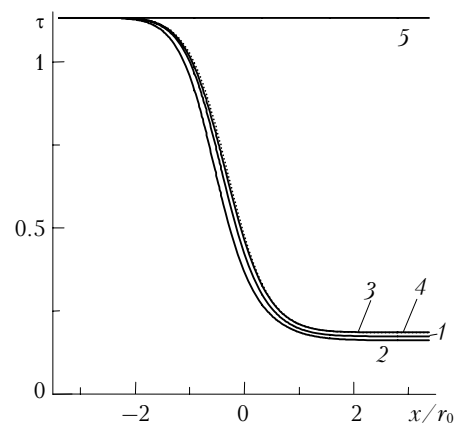


**Fig. 3.** Distribution of the aerosol layer optical thickness at the path end at  $N_\alpha = 0.2$  ( $\tau_0 = 1.133$ ),  $N_{v0} = 1$ :  $N_t = 1$ ,  $F = 2.59$  (1);  $N_t = 2$ ,  $F = 1.29$  (2);  $N_t = 0.5$ ,  $F = 5.18$  (3);  $N_t = 0$ ,  $F = 5.18$  (4);  $N_t = 0$ ,  $N_{v0} = 0$ ,  $F = 1.29$  (5).

The transparency function  $Tr(x, z = L) = I(x, L) / I(x, 0)$  changes significantly, as the thermal blooming effect increases (Fig. 4).

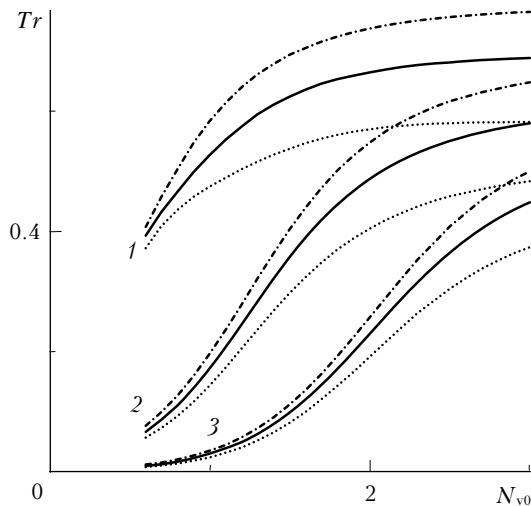


**Fig. 4.** Transparency of the cleared aerosol  $Tr = I(x = r_0, z = L)/I(r_0, 0)$  as a function of the clearing parameter  $N_{v0}$ . The initial optical thickness  $\tau_0 = 1$  (curve 1), 2 (2), 3 (3); the thermal-blooming parameter  $N_t = 1$  (solid curves), 2 (dashed curves), and 0.5 (dot-and-dash curves).

The results shown in Fig. 4 demonstrate that the clearing effect decreases as the initial optical thickness  $\tau_0$  grows, while it increases as  $N_{v0}$  grows.

The growth of the thermal-blooming parameter  $N_t$  and the decrease of the Fresnel number weaken the clearing effect. The same level of transparency is achieved at constant  $N_{v0}$  in a denser optical medium at smaller values of the thermal-blooming parameter.

#### 4. Comparison with the experiment

A satisfactory agreement with the experimental data has been obtained for the unsteady and steady-state clearing.<sup>3,15</sup> In the experiment,  $P_0 = 800$  W,  $\lambda = 10.6$  and  $0.57$   $\mu\text{m}$  for the clearing and sensing radiation,  $\tau_0 = 0.206$  (1.02 at  $\lambda = 0.57$   $\mu\text{m}$ ), 0.445 (1.91), 0.814 (2.95), 1.413 (4.27), 2.8 (6.57) (which corresponds to  $a_m = 1.75$ ; 1.75; 2.0; 2.5; and 3  $\mu\text{m}$ ,  $\mu = 5, 4, 4, 5, 5$ ) and  $r_0 = 0.02$  m,  $V_0 = 0.3$  m/s,  $L = 4$  m,  $p_\infty = 1$  atm,  $T_\infty = 293.15$  K. The similarity parameters are  $N_{v0} \approx 0.316$ ;  $F = 59.2$ ;  $N_t \approx 0.012$ – $0.140$ . The calculated levels of transparency  $Tr(x = r_0, z = L) = I(r_0, L)/I(r_0, 0)$ , for example, in the steady-state limit of the clearing process are:  $Tr(r_0) \approx 0.890$ ; 0.750; 0.526; 0.232 (at  $\tau_0 = 0.206$ ; 0.445; 0.814; 1.413) and well correspond to the experimental values<sup>3,15</sup>:  $Tr(r_0) \approx 0.924$ ; 0.829; 0.627; 0.365.

The approach developed allows a prediction and improvement of the results. For example, at  $\tau_0 = 1.413$  ( $\tau_{0.57} = 4.27$ ) the increase of the clearing parameter  $N_{v0}$  from 0.316 to 0.662 and 1.234 (at  $P_0 = 800$  W, only due to the change of the beam radius and air speed from  $r_0 = 0.02$  m,  $V_0 = 0.30$  to 0.0289; 0.0409 m and 0.0994; 0.0351 m/s) in the experiment gives a possibility to attain a significant increase in the transparency function of the cleared zone from  $Tr_0(r_0) = 0.232$ ,  $Tr_{0.57}(r_0) = 0.0586$  to  $Tr_0(r_0) = 0.523$ ; 0.811,  $Tr_{0.57}(r_0) = 0.17$ ; 0.387 at wavelengths of 10.6 and 0.57  $\mu\text{m}$ , respectively.

## Conclusions

The clearing of the polydisperse water aerosol increases with the increase of the dimensionless clearing parameter  $N_{v0}$  at the variation of the physical parameters of the problem (optical, mechanical, geometric, and energy ones) and the other similarity parameters kept constant.

The diffraction leads to the beam widening, the clearing increases the intensity peak at the path end and shifts the peak downward along the flux. The thermal blooming defocuses the beam and shifts it to meet the flux. The effects of shifting and increasing the peak grow with the increase of  $N_t$ . The thermal blooming significantly affects the transparency function and weakly influences relative variations of the optical thickness.

In the cases considered at the relatively slow diffusion and diffusion-convective vaporization of droplets, the increase of the thermal-blooming parameter  $N_t$  and the decrease of the Fresnel number weaken the clearing effect. The same level of transparency is achieved at constant  $N_{v0}$  in the optically denser medium at smaller values of the thermal-blooming parameter.

## Acknowledgments

This work was supported, in part, by ISTC Grant No. 2249 and Grant in Support of Scientific Schools NSH-1984.2003.

## References

1. F.A. Williams, *Int. J. Heat and Mass Transfer* **8**, No. 4, 575–590 (1965).
2. V.E. Zuev, Yu.D. Kopytin, and A.V. Kuzikovskii, *Nonlinear Optical Effects in Aerosols* (Nauka, Novosibirsk, 1980), 116 pp.
3. O.A. Volkovitskii, Yu.S. Sedunov, and L.P. Semenov, *Propagation of Intense Laser Radiation in Clouds* (Gidrometeoizdat, Leningrad, 1982), 312 pp.
4. V.E. Zuev, A.A. Zemlyanov, Yu.D. Kopytin, and A.V. Kuzikovskiy, *High-Power Laser Radiation in Atmospheric Aerosols* (D. Reidel, Amsterdam, 1985).
5. A.N. Kucherov, *Teplofiz. Vysok. Temperatur* **29**, No. 1, 144–152 (1991).
6. V.N. Lugovoi and A.M. Prokhorov, *Usp. Fiz. Nauk* **111**, No. 2, 203–247 (1973).
7. C.F. Bohren and D.R. Huffman, *Absorption and Scattering of Light by Small Particles* (Wiley, New York, 1983).
8. J. Knight, *AIAA Journal* **17**, No. 5, 519–523 (1979).
9. A.P. Sukhorukov and E.N. Shumilov, *Zh. Tekh. Fiz.* **43**, No. 5, 1029–1041 (1973).
10. A.N. Kucherov, *Atmos. Oceanic Opt.* **7**, No. 10, 749–752 (1994).
11. A.N. Kucherov, *Sov. J. Quant. Electron.* **25**, No. 3, 236–240 (1995).
12. R.L. Armstrong, *Appl. Opt.* **23**, No. 1, 148–155 (1984).
13. A.N. Kucherov, *Int. J. Heat and Mass Transfer* **43**, No. 15, 2793–2806 (2000).
14. M.N. Kogan and A.N. Kucherov, *Dokl. Akad. Nauk SSSR* **253**, No. 3, 575–577 (1980).
15. O.A. Volkovitskii and V.K. Mamonov, *Sov. J. Quant. Electron.* **7**, No. 5, 626–629 (1977).